Rolling and ordering of micro rods in shear flow induced by rod wall interactions.

Martin Wittmann[1], Igor M. Kulić[2], Antonio Stocco[2] and Juliane Simmchen[3]

[1]Physical Chemistry TU Dresden, Zellescher Weg 19, 01062 Dresden, Germany

[2]Institut Charles Sadron, CNRS UPR-22, 23 rue du Loess, Strasbourg, France.

[3]Pure and applied chemistry, University of Strathclyde, Cathedral Street, Glasgow, UK

October 29, 2024

S1 List of SI Videos

- SIVideo1_DifferentFlowSpeedsDIWater.avi - Glass rods in DI water at different flow rates (2.5 mL/h, 5 mL/h, 10 mL/h)
- SIVideo2_2.5mLperhNaCl.avi - Glass rods in a flow rate of 2.5 mL/h in different solvents (DI water, 10^{-5} M NaCl, 10^{-4} M NaCl)

S2 Determination of the Debye length

The Debye length λ_D is given by Equation S1 and is essential to predict the electrostatic interaction between rod and substrate.

$$\lambda_D = \kappa^{-1} = \left(\frac{e^2 N_A}{\varepsilon_0 \varepsilon_r k_B T} \sum_i c_i \right)^{-1/2} \tag{S1}$$

In the sum of the concentrations of ions present in the solution ($\sum_i c_i$) different contributions have to be considered:

- H^+ and OH^-: 10^{-7} M for each ion at pH 7 $\rightarrow 2 \times 10^{-7}$ M
- CO_2 from the ambient atmosphere forms H_2CO_3 and dissociates to H^+ and $HCO_3{}^-$ in the solution. The concentrations can be determined by measuring the electrical conductivity and using the molar conductivity
- The added NaCl with a known concentration

While the concentrations of H^+, OH^- and the added NaCl are known, the contribution from H^+ and $HCO_3{}^-$ from ambient CO_2 has to be determined, which can be done using the specific conductivity $\kappa_{conduct}$ of the solution. As the concentrations are very low, we can estimate, that $\kappa_{conduct} = c\Lambda_m^0$. Here, Λ_m^0 is the limiting molar conductivity at infinite dilution, which can be calculated from the limiting molar conductivities of the individual ions[1]:

$$\begin{aligned}
\Lambda_m^0(\mathrm{H^+ + HCO_3^-}) =& \lambda_m^0(\mathrm{H^+}) + \lambda_m^0(\mathrm{HCO_3^-}) \\
\Lambda_m^0(\mathrm{H^+ + HCO_3^-}) =& (349.65 + 44.5) \cdot 10^{-4}\ \mathrm{m^2S/mol} \\
\Lambda_m^0(\mathrm{H^+ + HCO_3^-}) =& 394.15 \cdot 10^{-4}\ \mathrm{m^2S/mol}
\end{aligned}$$

The DI water used in the experiments had a specific conductivity of $\kappa_{conduct} = 0.59$ µS/cm. Subtracting the specific conductivity of ultrapure water and dividing by the limiting molar conductivity, we get the concentration of H^+ and $HCO_3{}^-$ originating from ambient CO_2:

$$\begin{aligned}
c(\mathrm{H^+ + HCO_3^-}) =& \frac{\kappa_{conduct} - \kappa_{conduct}(ultrapure)}{\Lambda_m^0(\mathrm{H^+ + HCO_3^-})} \\
c(\mathrm{H^+ + HCO_3^-}) =& \frac{0.59\ \mu\mathrm{S/cm} - 0.055\ \mu\mathrm{S/cm}}{394.15 \cdot 10^{-4}\ \mathrm{m^2S/mol}} \\
c(\mathrm{H^+ + HCO_3^-}) =& 1.36 \cdot 10^{-6}\ \mathrm{mol/L}
\end{aligned}$$

The expected contribution of the conductivity of NaCl ($\Lambda_m^0(\mathrm{NaCl}) = 126.39 \cdot 10^{-4}$ m^{2}S/mol)[1] to the total specific conductivity can be estimated and the values are summarised in Table S1. Looking at the measured conductivity of the 10^{-6} M NaCl it is noteworthy, that measured conductivity shows a higher increase than expected purely from the contribution of NaCl. We explain this by a longer preparation process of the NaCl solutions, where they are exposed to ambient CO_2. Therefore, we assume this contribution for all concentrations of NaCl.

Table S1: Determination of Debye length using the specific conductivity.

Solution	$\kappa_{conduct}$ in µS/cm	$\kappa_{conduct}$(NaCl) in µS/cm	$c(CO_2)$ in µM	Debye length in nm
DI water	0.59	0	1.36	254
10^{-6} M NaCl	1.57	0.126	3.5	143
10^{-5} M NaCl	2.56	1.26	3.5	83
10^{-4} M NaCl	12.63	12.63	3.5	30

S3 Determination of the height.

S3.1 Measuring height using the velocity v

For a Poiseuille flow through square $H \times H$ cross-section in the x direction of a long channel and a given volumetric flow rate Q, pressure gradient $G = -\frac{dp}{dx}$ and viscosity η the flow field $u(y,z)$ is given by the following equation: (as derived by Boussinesq)[2]

$$u(y,z) = \frac{G}{2\eta} y(H-y) - \frac{4GH^2}{\eta\pi^3} \sum_{n=1}^{\infty} \frac{1}{(2n-1)^3} \frac{\sinh(\beta_n z) + \sinh[\beta_n (H-z)]}{\sinh(\beta_n H)} \sin(\beta_n y)$$

$$\beta_n = \frac{(2n-1)\pi}{H},$$

$$Q = \frac{GH^4}{\eta} \left(\frac{1}{12} - \frac{16}{\pi^5} \sum_{n=1}^{\infty} \frac{1}{(2n-1)^5} \frac{\cosh(\beta_n H) - 1}{\sinh(\beta_n H)} \right)$$

The relation for the flow rate can be approximated

$$Q \approx 0.035 \frac{GH^4}{\eta}$$

from which we can estimate pressure drop

$$G = 28.6\,\frac{\eta Q}{H^4} = 7.94\frac{Pa}{m}\cdot q$$

where $q = Q/\left(\frac{mL}{h}\right)$ is the non-dimensional flow rate.

We assume that we are close to the bottom in the z-direction, i.e. $z/H \ll 1$ very small, and to be in the centre of the channel in the y-direction, $y = \frac{H}{2}$, giving the velocity profile:

$$u(z) \approx 0.38\frac{GH^2}{\eta}\frac{z}{H} + O\left(z^2\right)$$

Replacing $G = 28.6\,\frac{\eta Q}{H^4}$ we obtain

$$u(z) = \dot{\gamma} z + O\left(z^2\right) \tag{S2}$$

with the (close to the wall) shear rate given by

$$\dot{\gamma} = 10.87\frac{Q}{H^3} \tag{S3}$$

Assuming that a rod in a shear flow is moving with the velocity of the fluid at its center of mass (z), the velocity v is given as:

$$v(z) = \dot{\gamma}\cdot z$$
$$z = h + r$$

Where h and r are the (surface-surface) height and the radius of the rod. The obtained data for the different concentrations of NaCl are summarized in Table S2.

Table S2: Height between rod and substrate measured using the velocity.

Solution	v at 5 mL/h in µm/s	z in nm	h in nm
DI water	36.8	2440	940
10^{-6} M NaCl	26.6	1760	260
10^{-5} M NaCl	23.5	1560	60
10^{-6} M NaCl	26.6	1030	-470

S3.2 Prediction of height considering the potential as the sum of electrostatic interaction and gravity

According to[3], the electrostatic interaction potential of a rod with a length L, radius r, a zeta potential ζ_{rod} and a height h with a wall with a zeta potential ζ_{wall} is given as:

$$U_E(h) = 64\pi LB\sqrt{\frac{\kappa r}{2\pi}}e^{-\kappa h} \tag{S4}$$

$$B = \varepsilon_0\varepsilon_r\left(\frac{k_BT}{e}\right)^2 \tanh\left(\frac{e\zeta_{rod}}{4k_BT}\right)\tanh\left(\frac{e\zeta_{wall}}{4k_BT}\right)$$

With a density mismatch between rod and solvent $\Delta\rho$ the gravitational potential is given as:

$$U_G(h) = \pi r^2 Lg\Delta\rho\, h$$

Balancing the two potentials (minimizing $U(h) = U_E + U_G$) we get

$$U'(h) = 0 = \pi r^2 Lg\Delta\rho - 64\pi LB\kappa\sqrt{\frac{\kappa r}{2\pi}}e^{-\kappa h}$$

$$h = \frac{1}{\kappa}\ln\left(\frac{64B\kappa\sqrt{\frac{\kappa a}{2\pi}}}{r^2 g\Delta\rho}\right) \tag{S5}$$

For $\zeta_{rod} = -36$ mV (experimental value), $\zeta_{wall} = -40$ mV (estimated value for glass), the Debye lengths κ^{-1} from Table S1 and $\Delta\rho = 1.6$ g/cm^3 we get the following heights summarized in Table S3.

Table S3: Height between rod and substrate predicted considering the potential as the sum of electrostatic interaction and gravity.

Solution	Debye length in nm	h in nm
DI water	254	1520
10^{-6} M NaCl	143	980
10^{-5} M NaCl	83	640
10^{-4} M NaCl	30	280

S3.3 Measuring height using the rotational diffusion

A micro rod near a wall shows translational diffusion in the perpendicular and parallel direction with respect to the rod long axis ($D_\perp$ and $D_\parallel$) and rotational diffusion parallel to the wall normal (D_{rot}), which are influenced by the presence of the nearby wall and therefore can be used to estimate the height. The rotational diffusion (D_{rot}) will be used here and a prediction from Hunt *et al.* was applied to quantify the influence of a wall on its magnitude.[4] There, the rotational friction coefficient near a wall (ξ_{rot}) is given as:

$$\xi_{rot} = \frac{4\pi\eta}{\cosh^{-1}(z/r)} \cdot \frac{L_1^3 + L_2^3}{3} \tag{S6}$$

Here, L_1 and L_2 are the distances of the ends from the rotation axis and if it is located at the centre of the rod we get $L_1 = L_2 = L/2$. z is the z-position of the center of mass and therefore $h = z - r$. The diffusion coefficient is given as: $D_{rot} = \dfrac{k_b T}{\xi_{rot}}$ which leads to Equation S7. As the used rods are only homogeneous in diameter but not in length we have to consider the length (Figure S1a) of the rod and determine the height by fitting the experimental data of $D_{rot}(L)$ to Equation S7 to get the height h. An example with data obtained in DI water is displayed in Figure S1b and results are summarized in Table S4.

$$D_{rot}(L) = \frac{3 \cdot \cosh^{-1}((h+r)/r) k_b T}{\pi\eta L^3} \tag{S7}$$

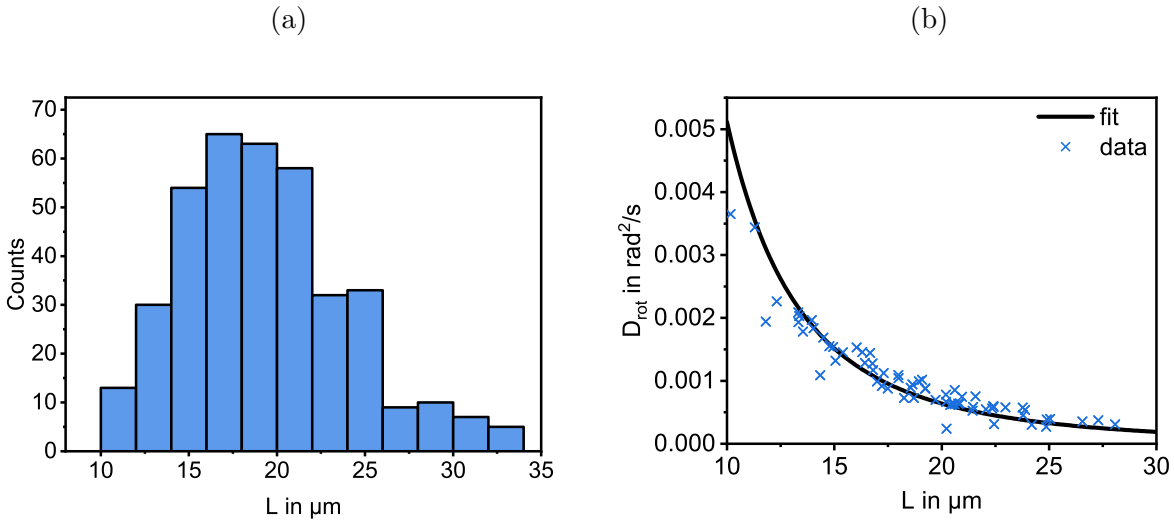

Figure S1: (a) Histogram of lengths of glass micro rods, (b) Experimental data of $D_{rot}(L)$ for glass rods in DI water with the corresponding fit ($h = 1070$ nm).

Table S4: Height between rod and substrate measured using the velocity.

Solution	$D_{rot}(L = 18\,\mu\text{m})$ in s^{-1}	h in nm
DI water	8.6×10^{-4}	1070
10^{-6} M NaCl	8.4×10^{-4}	1020
10^{-5} M NaCl	7.2×10^{-4}	730
10^{-4} M NaCl	5.3×10^{-4}	380

S4 The motion-angle - director-angle correlation

S4.1 Coupling between translation and rotation

Similar to the work of Teng *et al.*, the coupling between translation and rotation is given by the resistance matrix $\boldsymbol{R}$ (Equation S8).[5] Here, $F_\perp$ and N are the force in the orthogonal direction with respect to the long axis and the torque around the long axis, respectively. v and ω stand for the velocity orthogonal to the long axis and the angular velocity around the long axis, respectively.

$$\begin{pmatrix} F_\perp \\ N \end{pmatrix} = \begin{pmatrix} R_{11} & R_{12} \\ R_{21} & R_{22} \end{pmatrix} \begin{pmatrix} v \\ \omega \end{pmatrix} \tag{S8}$$

To get the velocity of a rod rotating at a certain height from the substrate, we apply a force-free rotation ($F_\perp = 0$) the resulting velocity is now:

$$v = -\frac{R_{12}}{R_{11}}\omega$$

We can fit the values for R_{12} and R_{11} derived by ref[5] using OpenFoam simulations as:

$$R_{11} = -\eta \left(\frac{4\pi}{\log\left(1 + \delta + \sqrt{2\delta + \delta^2}\right)} L + \frac{15\delta}{\delta + 0.005} r \right)$$
$$R_{12}(\delta) = \eta r^2 \frac{32}{3\pi} \log\left(\frac{0.114}{\delta} + 0.904\right)$$

Where, L and r are the length and radius of the rod, η is the viscosity and $\delta = h/r$. Looking at the resulting velocities normalized to perfect coupling ($\omega \cdot r$) (Figure S2), we get low values in the range of 10^{-3} to 10^{-2}, with a maximum at a height of 70 nm. Notably, the coupling becomes weaker with the increasing length of the rod, as it originates from end effects.

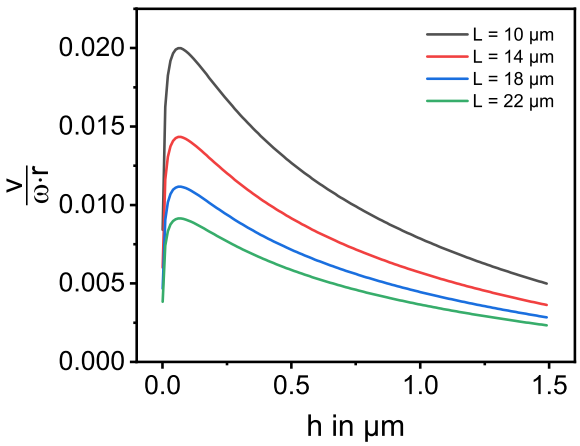

Figure S2: Velocity resulting from a force-free rotation of a rod with $r = 1.5$ µm and different lengths normalized on $\omega \cdot r$.

S4.2 Anisotropic mobility

Here, we investigate the origin of the non-trivial relation between the angle of motion β and the orientation angle α (with respect to the flow direction) in the shear flow. Assuming that the rod is approximately parallel to the substrate, its orientation vector (director) $\mathbf{t}$ is in the x-y plane and can be expressed in terms of the angle α:

$$\mathbf{t} = \begin{pmatrix} \sin\alpha \\ \cos\alpha \end{pmatrix}$$

The rod moves parallel to the surface with velocity components

$$\mathbf{v} = \begin{pmatrix} v_x \\ v_y \end{pmatrix}$$

and is acted upon by two types of forces:

1) **Bulk drag force**, coming from the mismatch of the rods velocity vector with the bulk flow (in the x-direction) in the rod plane

$$\mathbf{F}_{bulk-flow} = \left(\xi_{\perp}^{b}\left(\mathbf{I}-\mathbf{tt}\right)+\xi_{\parallel}^{b}\mathbf{tt}\right)\left(\mathbf{v}_b-\mathbf{v}\right)$$

$$\mathbf{v}_b = \begin{pmatrix} v_b \\ 0 \end{pmatrix} \text{ (bulk flow velocity)}$$

2) **Surface drag force**, coming from the close to surface lubrication contact.

$$\mathbf{F}_{surf} = \left(\xi_{\perp}^{s}\left(\mathbf{I}-\mathbf{tt}\right)+\xi_{\parallel}^{s}\mathbf{tt}\right)\left(0-\mathbf{v}\right)$$

where the 0 is the vanishing velocity of the wall. Here we introduce the unity operator $\mathbf{I}$ and matrix "$\mathbf{tt}$" $= \mathbf{t}\cdot\mathbf{t}^{\mathbf{T}}$ (T: the transpose), which is the projector operator onto the director $\mathbf{t}$. The two sets of friction coefficients $\left(\xi_{\perp}^{b},\xi_{\parallel}^{b}\right)$ and $\left(\xi_{\perp}^{s},\xi_{\parallel}^{s}\right)$ are the contributions coming from the

pure bulk hydrodynamic friction (b) and pure surface/lubrication contribution (s) respectively. Total force balance requires $\mathbf{0} = \mathbf{F}_{bulk-flow} + \mathbf{F}_{surf}$ which implies the relation

$$\mathbf{v} = \left(\left(\xi_{\perp}^{s} + \xi_{\perp}^{b}\right)(\mathbf{I} - \mathbf{tt}) + \left(\xi_{\parallel}^{s} + \xi_{\parallel}^{b}\right)\mathbf{tt}\right)^{-1}\left(\xi_{\perp}^{b}(\mathbf{I} - \mathbf{tt}) + \xi_{\parallel}^{b}\mathbf{tt}\right)\mathbf{v}_b$$

Using the usual laws for the projectors, $(\mathbf{I} - \mathbf{tt})(\mathbf{tt}) = 0$, $(\mathbf{tt})^2 = \mathbf{tt}$, $(\mathbf{I} - \mathbf{tt})^2 = \mathbf{I} - \mathbf{uu}$, the expression simplifies to

$$\begin{aligned}\mathbf{v} &= \left(\frac{\xi_{\perp}^{b}}{\xi_{\perp}^{s} + \xi_{\perp}^{b}}(\mathbf{I} - \mathbf{tt}) + \frac{\xi_{\parallel}^{b}}{\xi_{\parallel}^{s} + \xi_{\parallel}^{b}}\mathbf{tt}\right)\mathbf{v}_b \\ &= v_b\left(r_{\parallel} - r_{\perp}\right)\begin{pmatrix} \frac{r_{\perp}}{r_{\parallel} - r_{\perp}} + \sin^2\alpha \\ \cos\alpha\sin\alpha \end{pmatrix}\end{aligned}$$

with the two friction ratios $r_{\perp} = \frac{\xi_{\perp}^{b}}{\xi_{\perp}^{s}+\xi_{\perp}^{b}}$, $r_{\parallel} = \frac{\xi_{\parallel}^{b}}{\xi_{\parallel}^{s}+\xi_{\parallel}^{b}}$.
We see that when the surface friction can be neglected ($\xi_{\perp}^{s}, \xi_{\parallel}^{s} = 0$) we have the trivial solution $\mathbf{v} = \mathbf{v}_b$, i.e. as expected the rod moves with the flow speed and direction, regardless of its tangent $\mathbf{t}$.
Abbreviating

$$r_{fr} = \frac{r_{\perp}}{r_{\parallel} - r_{\perp}} = \frac{\xi_{\perp}^{b}\left(\xi_{\parallel}^{s} + \xi_{\parallel}^{b}\right)}{\xi_{\parallel}^{b}\left(\xi_{\perp}^{s} + \xi_{\perp}^{b}\right) - \xi_{\perp}^{b}\left(\xi_{\parallel}^{s} + \xi_{\parallel}^{b}\right)}$$

the motion angle w.r.t. the x-axis is then

$$\cos\beta = \frac{r_{fr} + \sin^2\alpha}{\sqrt{(2r_{fr} + 1)\sin^2\alpha + r_{fr}^2}} \tag{S9}$$

which is the relation used in the main text. Fitting the parameter r_{fr} to our experimental data, we get a value of $r_{fr} = 38$ in DI water and smaller values down to $r_{fr} = 13$ with increasing concentration of NaCl (Figure S3).

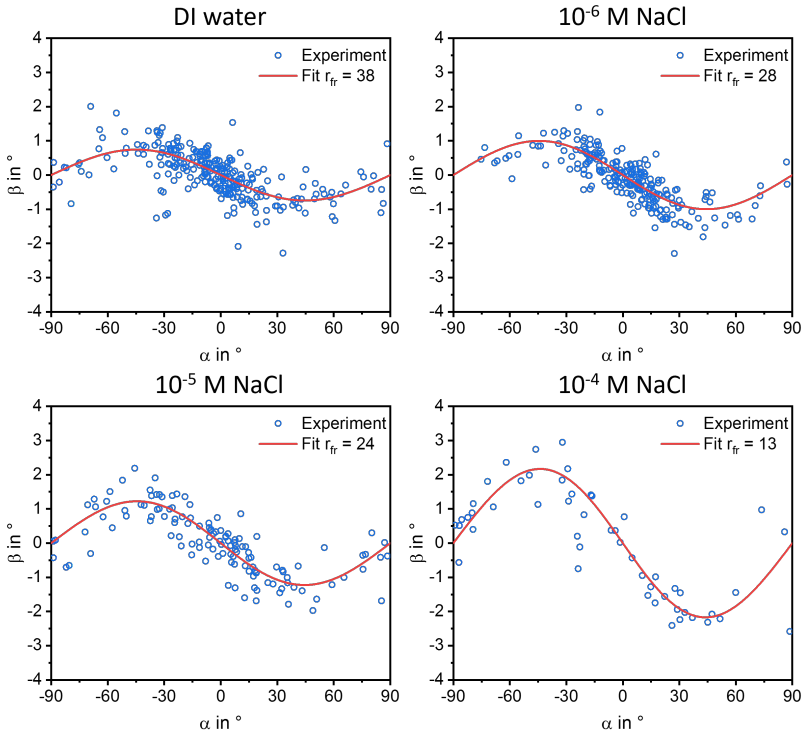

Figure S3: Relation between the rod orientation angle α and the angle of motion direction β at a flow rate of 2.5 mL/h in DI water and NaCl with a fit using Equation S9.

S5 Tilting potential of the rod near wall

Before, the height of a rod was determined considering an orientation parallel to the wall. If we allow now for a slight tilt and introduce a tilting angle τ, the rods total energy is given by Equation S10 with an interaction potential $w(h)$ density per unit length integrated over the full length L, where the integral goes over the arc length of the rod s.

$$W(h,\tau) = \int_{-L/2}^{+L/2} w(h + s\sin(\tau))\, ds \tag{S10}$$

Assuming a small tilting angle τ we can Taylor expand $w(h + s\sin(\tau)) \approx w(h) + w'(h)\, s\sin(\tau) + \frac{1}{2} w''(h)\, s^2 \sin^2(\tau)$ and the energy simplifies

$$W(h,\tau) = Lw(h) + w''(h)\sin^2(\tau)\frac{L^3}{24} \tag{S11}$$

Specializing now to the electrostatic potential of a rod near a wall (Equation S4) we get:

$$w(h) = \frac{U_E(h)}{L} = 64\pi B\sqrt{\frac{\kappa r}{2\pi}}e^{-\kappa h}$$

with the second derivative

$$w''(h) = 64\pi\kappa^2 B\sqrt{\frac{\kappa r}{2\pi}}e^{-\kappa h}$$

The harmonic stiffness constant a of the tilting variable is finally given as:

$$a = \frac{w''(h)\,L^3}{12}$$

$$a = \frac{16\pi\kappa^2 BL^3}{3}\sqrt{\frac{\kappa r}{2\pi}}e^{-\kappa h}$$

If we now insert Equation S5 for h depending on κ we get:

$$a = \frac{\kappa\pi r^2 g\Delta\rho L^3}{12} \tag{S12}$$

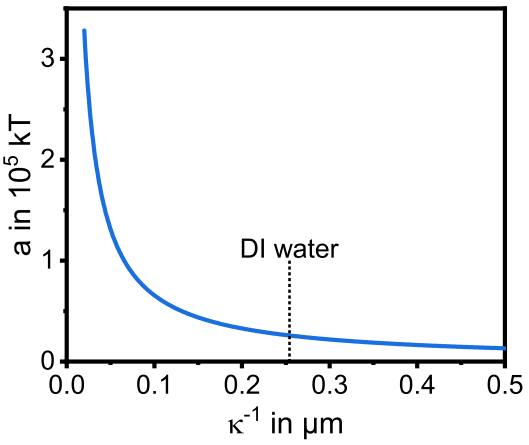

Figure S4: Plot of a vs. the Debye length κ^{-1} according to Equation S12.

S6 Simulation of orientation of rods in shear flow near a wall

S6.1 Interaction with flow and wall

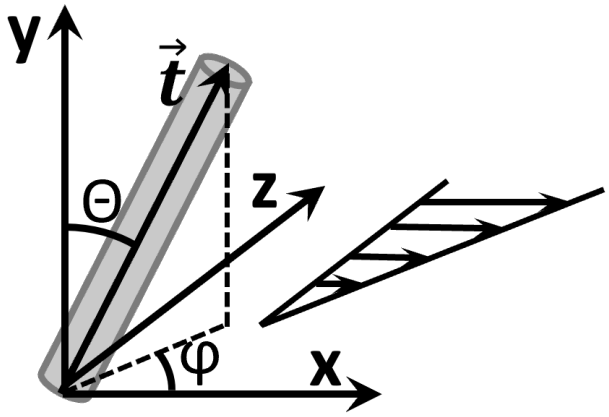

Figure S5: Coordinate system with definition of angles Θ (angle to y-axis) and Φ (angle of projection of **u** on x-y plane). The flow goes in the x-direction, the gradient in the z-direction, and the wall is in the x-y plane.

In a simple shear flow, next to the wall, we have a combination of two effects: The torque $\mathbf{M}_{wall}$ caused by the electrostatic wall-rod interaction and the hydrodynamic torque, $\mathbf{M}_{hydr}$, coming from the shear flow itself.

S6.1.1 The wall torque

The wall-induced torque is a vector orthogonal to the rod director $\mathbf{t}$ and the plane unit normal $\hat{\mathbf{z}}$.

$$\mathbf{M}_{wall} = M_{wall}\, \mathbf{t} \times \hat{\mathbf{z}}$$

Its magnitude can be derived from the tilting angle related potential, Eq. S11 from the previous section

$$M_{wall} = -\frac{\partial}{\partial \tau} W(h, \tau)$$
$$\approx -a(h)\,\tau$$

where $\tau \ll 1$ is assumed to be small and $a(h)$ is the stiffness constant from Eq. S12. In terms of the rod director components

$$\mathbf{t} = \begin{pmatrix} t_x \\ t_y \\ t_z \end{pmatrix}$$

the tilt angle τ can be also expressed as

$$\tau \approx t_z = \sqrt{1 - t_x^2 - t_y^2}$$

S6.1.2 Hydrodynamic torque

Following Dhont and Briels,[6], the time evolution of the rod director $\mathbf{t}(t)$ in the simple shear flow can be described in terms of its angular velocity vector $\boldsymbol{\omega}(t)$

$$\frac{d\mathbf{t}}{dt} = \boldsymbol{\omega} \times \mathbf{t}$$

Given the angular velocity, the hydrodynamic torque is then given by

$$\mathbf{M}_{hydr} = -\xi_{rot}\left[\boldsymbol{\omega} - \hat{\mathbf{t}} \times \left(\boldsymbol{\Gamma} \cdot \hat{\mathbf{t}}\right) + \varepsilon^2 \hat{\mathbf{u}} \times \left(\boldsymbol{\Gamma}^{\boldsymbol{T}} \cdot \hat{\mathbf{t}}\right)\right]$$

where

$$\Gamma = \dot{\gamma} \begin{pmatrix} 0 & 0 & 1 \\ 0 & 0 & 0 \\ 0 & 0 & 0 \end{pmatrix}$$

is the velocity-gradient tensor for the simple shear flow, $\mathbf{\Gamma^T}$ its transpose and with the two constants ε and ξ_{rot}.

$$\varepsilon^2 = \frac{3}{2}\left(\frac{2r}{L}\right)^2 \log\left(\frac{L}{2r}\right) \text{ (hydrodynamic aspect ratio)}$$
$$\xi_{rot} = \frac{k_B T}{D_{rot}} \text{ (rotational friction coefficient)}$$

S6.1.3 Equation of motion

Balancing the surface torque with the hydrodynamic torque $\mathbf{M}_{wall} = \mathbf{M}_{hydr}$ gives the equations of motion for $\boldsymbol{\omega}$ and $\mathbf{t}$

$$-a\tau\,\hat{\mathbf{t}} \times \hat{\mathbf{z}} = -\xi_{rot}\left[\boldsymbol{\omega} - \hat{\mathbf{t}} \times \left(\mathbf{\Gamma} \cdot \hat{\mathbf{t}}\right) + \varepsilon^2 \hat{\mathbf{t}} \times \left(\mathbf{\Gamma^T} \cdot \hat{\mathbf{t}}\right)\right]$$
$$\frac{d\mathbf{t}}{dt} = \boldsymbol{\omega} \times \mathbf{t}$$

Solving the first one for $\boldsymbol{\omega}$ and inserting into the second one

$$\frac{d\mathbf{t}}{dt} = \left(\hat{\mathbf{t}} \times \left[\left(\mathbf{\Gamma} \cdot \hat{\mathbf{t}}\right) - \varepsilon^2\left(\mathbf{\Gamma^T} \cdot \hat{\mathbf{t}}\right) + \frac{a}{\xi_{rot}}\tau\,\hat{\mathbf{z}}\right]\right) \times \mathbf{t}$$

or split in components:

$$\frac{d}{dt}\begin{pmatrix} t_x \\ t_y \\ t_z \end{pmatrix} = \begin{pmatrix} \dot{\gamma} t_z \\ 0 \\ \frac{a}{\xi_{rot}} t_z - \varepsilon^2 \dot{\gamma} t_x \end{pmatrix} - t_z \left(\dot{\gamma} t_x \left(1 - \varepsilon^2\right) - \frac{a}{\xi_{rot}} t_z \right) \begin{pmatrix} t_x \\ t_y \\ t_z \end{pmatrix}$$

It seems that the equations for t_x and t_z decouple from t_y:

$$\dot{t}_x = \left(\dot{\gamma} - \dot{\gamma} t_x^2 \left(1 - \varepsilon^2\right) + \frac{a}{\xi_{rot}} t_z t_x \right) t_z \tag{S13}$$

$$\dot{t}_z = -\varepsilon^2 \dot{\gamma} t_x - \frac{a}{\xi_{rot}} t_z - t_z^2 \left(\dot{\gamma} t_x \left(1 - \varepsilon^2\right) - \frac{a}{\xi_{rot}} t_z \right) \tag{S14}$$

S6.1.4 Steady state solutions and their stability

The full phase plane is displayed in Figure S6, with a trivial equilibrium point for $t_x = 0$ and $t_z = 0$ corresponding to the preferred orientation observed in the experiment. Additionally, there are two saddle points close to $t_x = \pm 1$.

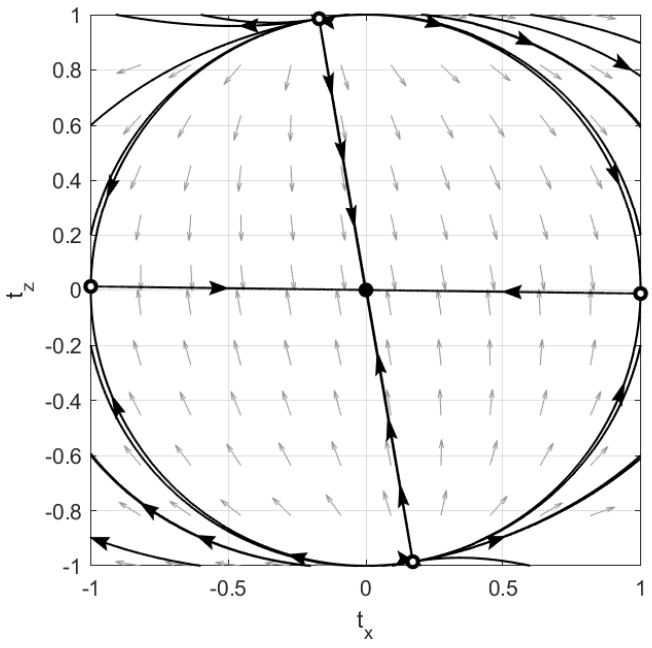

Figure S6: The (full non-linear system) (t_x, t_z) phase plane with $\xi_{rot} = 1150$ k_BTs, $\dot{\gamma} = 15$ s^{-1}, $\varepsilon = 0.273$ and $a = 100000$ k_BT.[7]

S6.1.5 Stability of the origin

In the following to proceed, we consider the $t_{x/z}$ system and drop the small $O\left(t_z^2\right)$ terms:

$$\dot{t}_x = \dot{\gamma}\left(1 - t_x^2\left(1-\varepsilon^2\right)\right)t_z \tag{S15}$$

$$\dot{t}_z = -\varepsilon^2\dot{\gamma}t_x - \frac{a}{\xi_{rot}}t_z \tag{S16}$$

Scaling all by $\dot{\gamma}$

$$\dot{\gamma}^{-1}\dot{t}_x = \left(1 - t_x^2\left(1-\varepsilon^2\right)\right)t_z$$

$$\dot{\gamma}^{-1}\dot{t}_z = -\varepsilon^2 t_x - \frac{a}{\xi_{rot}\dot{\gamma}}t_z$$

which we rewrite in the non-dimensional form

$$\dot{t}_x = \left(1 - t_x^2\left(1-\varepsilon^2\right)\right)t_z$$

$$\dot{t}_z = -\varepsilon^2 t_x - \alpha t_z$$

$$[Time] = \dot{\gamma}^{-1} \text{ (unit time)}$$

$$\alpha = \frac{a}{\xi_{rot}\dot{\gamma}}, \text{(scaled tilt-potential stiffness)}$$

$$\varepsilon^2 = \frac{3}{2}\left(\frac{2r}{L}\right)^2 \log\left(\frac{L}{2r}\right) \text{ (hydrodyn. aspect ratio)}$$

Small $u_z \ll 1$ approximation: As mentioned before, the origin $(t_x, t_z) = 0$ is an equilibrium point. To look at its stability, we need the corresponding eigenvalues of the linearized version of the rhs:

$$\dot{t}_x \approx t_z \text{ (linearized)}$$

$$\dot{t}_z \approx -\varepsilon^2 t_x - \alpha t_z$$

$$\frac{d}{dt}\begin{pmatrix} t_x \\ t_z \end{pmatrix} \approx \underbrace{\begin{pmatrix} 0 & 1 \\ -\varepsilon^2 & -\alpha \end{pmatrix}}_{\mathbf{A}} \begin{pmatrix} t_x \\ t_z \end{pmatrix}$$

with a matrix **A** representing the linear part of the dynamical system (around $(0,0)$). Its eigenvalues are

$$\lambda_{1/2} = -\frac{\alpha}{2} \pm \sqrt{\left(\frac{\alpha}{2}\right)^2 - \varepsilon^2}$$

When $\alpha, \varepsilon > 0$ they both have a negative real part which implies the stability of the origin. There are however two cases that manifest differently in terms of the observable motion (e.g. kayaking):

1. Case 1 (stiff tilt potential), $\alpha \geq 2\varepsilon$: Here we have two negative and real eigenvalues. The origin is an attractive node. There is no observable kayaking i.e. **no oscillation**, just relaxation.

2. Case 2 (soft potential) , $\alpha < 2\varepsilon$: The root $\sqrt{}$ becomes now imaginary and we have two complex conjugate eigenvalues:

$$Re\left(\lambda_{1/2}\right) = -\frac{\alpha}{2}$$
$$Im\left(\lambda_{1/2}\right) = \pm\sqrt{\varepsilon^2 - \left(\frac{\alpha}{2}\right)^2}$$

   The latter means that we have a **"relaxational kayaking"** that eventually dies out. The period of the kayaking is given as: $T_o = \frac{2\pi}{\sqrt{\varepsilon^2 - \left(\frac{\alpha}{2}\right)^2}}$.

The second case is particularly interesting if we have additional (thermal) excitations away from the equilibrium point.

S6.2 Adding thermal noise to the system

To introduce Langevin thermal dynamics we add a Gaussian white noise term $\sqrt{2k_BT/\xi_{rot}}\,\mathbf{N}_\omega$ to the angular velocity equation and the system now reads

$$\boldsymbol{\omega} = \hat{\mathbf{t}} \times \left[\xi_{rot} \left(\boldsymbol{\Gamma} \cdot \hat{\mathbf{t}} \right) - \xi_{rot} \varepsilon^2 \left(\boldsymbol{\Gamma}^{\boldsymbol{T}} \cdot \hat{\mathbf{t}} \right) + \frac{a\tau}{\xi_{rot}} \hat{\mathbf{z}} \right] + \sqrt{2k_B T / \xi_{rot}} \, \mathbf{N}_\omega$$
$$\frac{d\hat{\mathbf{t}}}{dt} = \boldsymbol{\omega} \times \hat{\mathbf{t}}$$

with the noise vector components $N_{\omega,i}$ $(i = 1, 2, 3)$

$$\langle N_{\omega,i}(t_1) \, N_{\omega,j}(t_2) \rangle = \delta_{ij} \delta(t_1 - t_2)$$

where the prefactor of the noise term, $\sqrt{2k_B T / \xi_{rot}}$, is chosen to satisfy the fluctuation dissipation relation. Inserting one into the other we get:

$$\frac{d\hat{\mathbf{t}}}{dt} = \hat{\mathbf{t}} \times \left[\xi_{rot} \left(\boldsymbol{\Gamma} \cdot \hat{\mathbf{t}} \right) - \xi_{rot} \varepsilon^2 \left(\boldsymbol{\Gamma}^{\boldsymbol{T}} \cdot \hat{\mathbf{t}} \right) + \frac{a\tau}{\xi_{rot}} \hat{\mathbf{z}} \right] \times \hat{\mathbf{t}} + \sqrt{2k_B T / \xi_{rot}} \, \mathbf{N}_\omega \times \mathbf{t}$$

Note that now the noise term on the r.h.s. becomes multiplicative noise, i.e. its amplitude depends on components of $\mathbf{t}$ itself

$$\mathbf{N}_\mathbf{t} = \begin{pmatrix} N_x \\ N_y \\ N_z \end{pmatrix} = \mathbf{N}_\omega \times \mathbf{t} = \begin{pmatrix} N_{\omega,1} \\ N_{\omega,2} \\ N_{\omega,3} \end{pmatrix} \times \begin{pmatrix} t_x \\ t_y \\ t_z \end{pmatrix} = \begin{pmatrix} N_{\omega,2} t_z - N_{\omega,3} t_y \\ N_{\omega,3} t_x - N_{\omega,1} t_z \\ N_{\omega,1} t_y - N_{\omega,2} t_x \end{pmatrix}$$

With this multiplicative noise term, the two dynamic equations for t_x and t_z read

$$\dot{t}_x = \left(\dot{\gamma} - \dot{\gamma} t_x^2 \left(1 - \varepsilon^2 \right) + \frac{a}{\xi_{rot}} t_z t_x \right) t_z + N_x$$
$$\dot{t}_z = -\varepsilon^2 \dot{\gamma} t_x - \frac{a}{\xi_{rot}} t_z - t_z^2 \left(\dot{\gamma} t_x \left(1 - \varepsilon^2 \right) - \frac{a}{\xi_{rot}} t_z \right) + N_z$$

Note that the equation for the y component $t_y = \sqrt{1 - (t_x^2 + t_z^2)}$ is entirely slaved by the two others and the normalization condition for the unit director $\mathbf{t}$.

S6.3 Scaled form of equations for simulation

We implement a Python simulation based on the Langevin system above. For that we scale all by $\dot{\gamma}$

$$\frac{d}{d\hat{t}}t_x = \left(1 - t_x^2\left(1-\varepsilon^2\right) + \alpha t_z t_x\right)t_z + \underbrace{\frac{N_x}{\dot{\gamma}}}_{n_x}$$

$$\frac{d}{d\hat{t}}t_z = -\varepsilon^2 t_x - \alpha t_z - t_z^2\left(t_x\left(1-\varepsilon^2\right) - \alpha t_z\right) + \underbrace{\frac{N_z}{\dot{\gamma}}}_{n_z}$$

$$N_x = \sigma\left(N_{\omega,2}t_z - N_{\omega,3}t_y\right)$$

$$N_y = \sigma\left(N_{\omega,3}t_x - N_{\omega,1}t_z\right)$$

$$N_z = \sigma\left(N_{\omega,1}t_y - N_{\omega,2}t_x\right)$$

$$\left\langle N_{\omega,i}\left(t_1\right)N_{\omega,j}\left(t_2\right)\right\rangle = \delta_{ij}\delta\left(\hat{t}_1 - \hat{t}_2\right)$$

$$\sigma^2 = \frac{2k_BT}{\xi_{rot}\dot{\gamma}}$$

$$\hat{t} = t/t_s = t\dot{\gamma}$$

where the dimensionless time $\hat{t}$ is now measured in units of inverse shear rate $t_s = 1/\dot{\gamma}$, and the stiffness a is given by the dimensionless parameter $\alpha = \frac{a}{\xi_{rot}\dot{\gamma}}$. We can experimentally determine ξ_{rot} using the data used to measure the height from the rotational diffusion coefficient. For a rod length $L = 18$ µm in DI water, we get $\xi_{rot} = 1150$ k_BTs which is used in the Python simulation.

References

[1] W. Haynes, *CRC Handbook of Chemistry and Physics, 94th Edition*, CRC Press, 2016.

[2] J. Boussinesq, *J. Math. Pures Appl.*, 1868, **2**, 377–424.

[3] J. L. Bitter, Y. Yang, G. Duncan, H. Fairbrother and M. A. Bevan, *Langmuir*, 2017, **33**, 9034–9042.

[4] A. J. Hunt, F. Gittes and J. Howard, *Biophysical journal*, 1994, **67**, 766–781.

[5] J. Teng, B. Rallabandi, H. A. Stone and J. T. Ault, *Journal of Fluid Mechanics*, 2022, **938**, A30.

[6] J. K. G. Dhont and W. J. Briels, in *Rod-Like Brownian Particles in Shear Flow: Sections 3.1 – 3.9*, John Wiley & Sons, Ltd, 2005, ch. 3a, pp. 147–216.

[7] Y. Zhang, *Yu Zhang (2024). Phase Portrait Plotter on 2D phase plane*, https://www.mathworks.com/matlabcentral/fileexchange/110785-phase-portrait-plotter-on-2d-phase-plane, Accessed: 2024-07-24.